

lncRNA UCA1 Mediates Resistance to Cisplatin by Regulating the miR-143/FOSL2-Signaling Pathway in Ovarian Cancer

Zewu Li,¹ Huanfu Niu,¹ Qianqian Qin,¹ Sanhui Yang,² Qin Wang,¹ Chunna Yu,¹ Zefeng Wei,¹ Zhenzhen Jin,¹ Xuenan Wang,¹ Aijun Yang,¹ and Xiaoli Chen¹

¹Center for Reproductive Medicine, Affiliated Hospital of Jining Medical University, Jining Medical University, Jining, China; ²Center for Clinical Skills Training, Affiliated Hospital of Jining Medical University, Jining Medical University, Jining, China

The aim of this study was to explore the roles of the long non-coding RNA (lncRNA) urothelial carcinoma-associated 1 (UCA1) on cisplatin resistance in ovarian cancer and the underlying mechanisms. We investigated the expression of lncRNAs in 3 paired cisplatin-sensitive and cisplatin-resistant tissues of ovarian cancer by microarray analysis. The qRT-PCR analysis was to investigate the expression pattern of UCA1 in cisplatin-resistant ovarian cancer patient tissues and cell lines. Then we examined the effects of UCA1 on cisplatin resistance *in vitro* and *in vivo*. In this study, UCA1 was observed to be upregulated in cisplatin-resistant patient tissues and cell lines. Knockdown of UCA1 inhibited cell proliferation and promoted the cisplatin-induced cell apoptosis in ovarian cancer cells. Then we demonstrated that repressed UCA1 promoted the miR-143 expression and miR-143 could bind to the predicted binding site of UCA1. Furthermore, we found that miR-143 displayed its role via modulating the FOSL2 expression. Importantly, we demonstrated that UCA1 was upregulated in serum exosomes from cisplatin-resistant patients. In summary, our study demonstrated that UCA1 modulates cisplatin resistance through the miR-143/FOSL2 pathway in ovarian cancer.

INTRODUCTION

Ovarian cancer is the most frequent cause of mortality among gynecological malignancies, usually diagnosed at an advanced metastatic stage.¹ The first-line therapy for ovarian cancer includes cytoreductive surgery and combined cisplatin-based chemotherapy. Although improvement in median survival has been observed in recent years, most patients eventually succumb to recurrent, progressive disease due to resistance to chemotherapy.² Evidence has shown that cisplatin resistance is a process with multifactorial participation that may originate through a series of modifications; however, the mechanism responsible for chemoresistance in ovarian cancer remains little understood.

Long noncoding RNAs (lncRNAs) are novel regulators of gene expression involved in the regulation of many cellular processes, including tumor growth and development, apoptosis, proliferation,

differentiation, and cell autophagy, and, therefore, they are implicated in cancers and other diseases.³ lncRNA UCA1 (urothelial carcinoma-associated 1) regulates the Wnt pathway through interacting with DNA, mRNA, microRNA (miRNA), and protein, thus affecting the biological activities of tumors.⁴ UCA1 was found to be increased in various types of cancers.^{5,6} However, there is no information pertaining to whether UCA1 is implicated in the cisplatin resistance of ovarian cancer.

Here, we showed that UCA1 was increased in cisplatin-resistant ovarian cancer tissues and cell lines. Further studies demonstrated that UCA1 affected the sensitivity of ovarian cancer cells to cisplatin. Our findings provide new insights into the regulatory mechanisms of UCA1 in the tumorigenesis and cisplatin resistance of ovarian cancer.

RESULTS

UCA1 Is Significantly Upregulated in Cisplatin-Resistant Ovarian Cancer Patient Tissues and Cell Lines

By using the cisplatin-sensitive and cisplatin-resistant tissues of ovarian cancer, we performed an lncRNA microarray assay to identify the dysregulated lncRNAs between them. The heatmap showed significant differentially expressed lncRNAs between cisplatin-sensitive and cisplatin-resistant tissues of ovarian cancer (Figure 1A), which were then subjected to validation by qRT-PCR. From the five upregulated lncRNAs validated in the first-round qRT-PCR experiments, we found that interference with the expression of lncRNA UCA1 reversed cisplatin resistance in both A2780-DDP and SKOV-3-DDP cell lines, while the other four lncRNAs showed little effect (Figure 1B; $p < 0.01$). Hence, we focused on the functional role of lncRNA UCA1.

To investigate the clinical significance of UCA1 expression in cisplatin sensitivity of ovarian cancer patients, the UCA1 expression

Received 19 March 2019; accepted 9 May 2019;
<https://doi.org/10.1016/j.omtn.2019.05.007>.

Correspondence: Xiaoli Chen, Center for Reproductive Medicine, Affiliated Hospital of Jining Medical University, Jining Medical University, Jining 272029, China.

E-mail: profzhjl@yeah.net



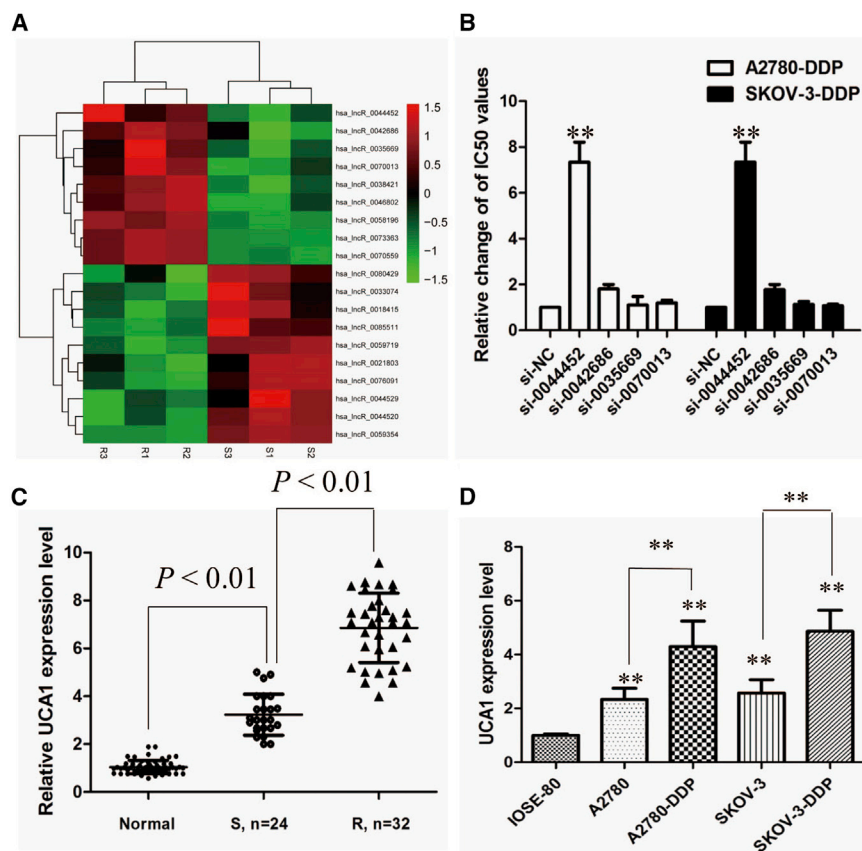


Figure 1. UCA1 Is Preferentially Upregulated in Cisplatin-Resistant Ovarian Cancer Patient Tissues

(A) lncRNA microarray data of three-paired cisplatin-resistant ovarian cancer and cisplatin-sensitive ovarian cancer are presented in a heatmap. (B) Determination of half maximal inhibitory concentration (IC_{50}) values of cisplatin for both resistant cell lines after transfection with various siRNAs. (C) Relative expression of UCA1 in cisplatin-resistant ovarian cancer and cisplatin-sensitive ovarian cancer. (D) Relative expression of UCA1 in a panel of ovarian cancer cell lines. All tests were performed at least three times. Data were expressed as mean \pm SD. *** $p < 0.001$, ** $p < 0.01$.

ectopic overexpression of UCA1 by transfecting A2780 and SKOV-3 cell lines with pcDNA-UCA1 expression vector (Figures S1C and S1D; $p < 0.01$).

UCA1 silencing suppressed the proliferation of resistant ovarian cancer cells after exposure to cisplatin (20 μ M) (Figures 2A and 2B; $p < 0.01$), implying that UCA1 promotes the proliferation of resistant ovarian cancer cells. After overexpression of UCA1, the growth rates of A2780 and SKOV-3 cells were significantly increased compared to the control group (Figures 2C and 2D; $p < 0.01$). To further confirm the effect of UCA1 on cisplatin resistance, we analyzed the rate of apoptosis using annexin

V-allophycocyanin (APC)/DAPI double staining and flow cytometry. Silencing of UCA1 promoted the cisplatin-induced cell apoptosis of resistant ovarian cancer after exposure to cisplatin (20 μ M) (Figure 2E; $p < 0.01$). However, cell apoptosis assays revealed that overexpression of UCA1 significantly decreased the apoptosis of A2780 and SKOV-3 cells after exposure to cisplatin (20 μ M) compared to the control group ($p < 0.01$; Figure 2F).

in normal ovarian tissues and ovarian cancer tissues from cisplatin-resistant and cisplatin-sensitive patients was analyzed. There was an increasing trend in UCA1 levels from normal ovarian tissues to cisplatin-sensitive ovarian cancer tissues and then to cisplatin-resistant ovarian cancer tissues, and the differences among the three groups were significant (Figure 1C; $p < 0.01$). Then, experiments were performed at the cellular level. The results showed that UCA1 expression was distinctively elevated in resistant ones and obviously lower in normal ovarian surface epithelial cells IOSE-80 (Figure 1D; $p < 0.01$).

lncRNA UCA1 Is Required for Cisplatin Resistance in Ovarian Cancer Cells

To further validate the relationship between UCA1 expression level and cisplatin resistance, we performed loss- and gain-of-function studies by knocking down or overexpressing UCA1 in ovarian cancer cells. A2780-DDP and SKOV-3-DDP cells were transfected with UCA1 small interfering RNAs (siRNAs) (respectively, si-UCA1#1, si-UCA1#2, and si-UCA1#3) or empty vectors (si-negative control [NC]). We detected UCA1 expression at 48 h post-transfection by qRT-PCR analysis to analyze knockdown efficiency, and we found that si-UCA1#1 had a higher efficiency of interference than the si-UCA1#2 and #3 groups (Figures S1A and S1B; $p < 0.01$), so we chose si-UCA1#1 for the subsequent experiments. Meanwhile, we induced

lncRNA UCA1 Facilitates Cisplatin Resistance of Ovarian Cancer *In Vivo*

To determine the effect of UCA1 on cisplatin resistance *in vivo*, SKOV-3 cells stably transfected with lentivirus vector containing UCA1 plasmid (Lv-UCA1) or NC (Lv-NC) were injected into the flanks of nude mice. According to the treatment, the tumors on the mice were actually assigned to the following groups: group 1, Lv-UCA1-transfected cells + cisplatin; group 2, Lv-UCA1-transfected cells + normal saline (NS); group 3, Lv-NC-transfected cells + cisplatin; and group 4, Lv-NC-transfected cells + NS.

The results showed that cisplatin treatment significantly inhibited the growth of tumor cells when compared with control groups (group 1 versus group 2 and group 3 versus group 4, respectively; Figures 3A and 3B). More importantly, with cisplatin treatment, tumor cells infected with Lv-UCA1 grew faster than controls (group 1

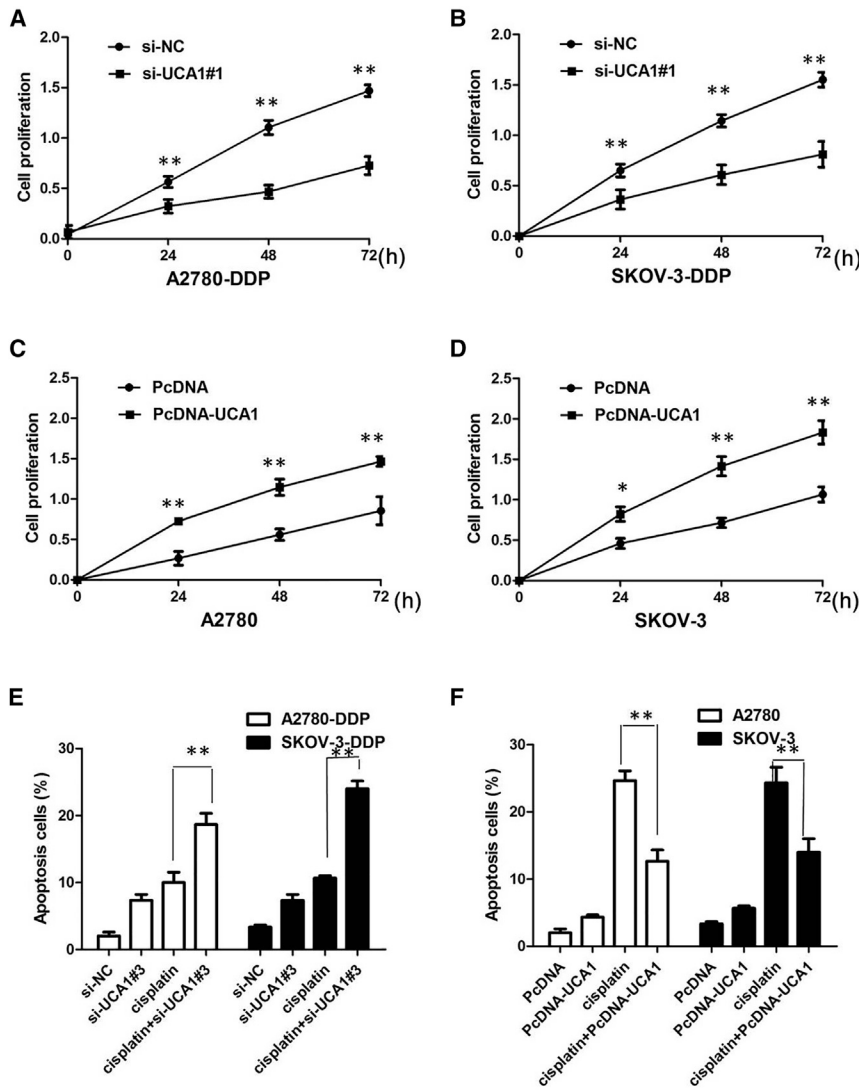


Figure 2. UCA1 Affects the Proliferation and Apoptosis of Ovarian Cancer *In Vitro*

(A) CCK-8 assay showing UCA1 silencing suppressed the proliferation of A2780-DDP cells in the presence of 4 $\mu\text{g}/\text{mL}$ cisplatin. (B) CCK-8 assay showing UCA1 silencing suppressed the proliferation of SKOV-3-DDP cells in the presence of 4 $\mu\text{g}/\text{mL}$ cisplatin. (C) CCK-8 assay showing the overexpression of UCA1 promoted the proliferation of A2780 cells in the presence of 4 $\mu\text{g}/\text{mL}$ cisplatin. (D) CCK-8 assay showing the overexpression of UCA1 promoted the proliferation of SKOV-3 cells in the presence of 4 $\mu\text{g}/\text{mL}$ cisplatin. (E) Flow cytometry analysis of apoptosis in A2780-DDP and SKOV-3-DDP cells transfected with si-Control or si-UCA1 prior to the stimulation of 4 $\mu\text{g}/\text{mL}$ cisplatin. (F) Flow cytometry analysis of apoptosis in A2780 and SKOV-3 cells transfected with pcDNAControl or pcDNA-UCA1 prior to the stimulation of 4 $\mu\text{g}/\text{mL}$ cisplatin treatment. All tests were performed at least three times. Data were expressed as mean \pm SD. ** $p < 0.01$.

To further validate the interaction, the UCA1 sequence containing the putative or mutated miR-143-binding site was cloned into the downstream of the luciferase reporter gene, generating wild-type (WT)-UCA1 and UCA1-MUT luciferase reporter plasmids. Then the effect of miR-143 on UCA1-WT and UCA1-MUT luciferase reporter systems was determined. The results showed that miR-143 mimic considerably reduced the luciferase activity of the UCA1-WT luciferase reporter vector compared with the NC, while the miR-143 mimic did not have any impact on the luciferase activity of UCA1-MUT-transfected cells (Figure 4B; $p < 0.01$). In a further RNA immunoprecipitation (RIP) experiment, UCA1 and miR-143 simultaneously existed in the production precipitated by anti-AGO2 (Figure 4C;

versus group 3), suggesting that UCA1 repressed the cell cytotoxicity induced by treatment with cisplatin *in vivo*. Moreover, immunohistochemistry assay showed that the tumors treated with Lv-UCA1 plus cisplatin displayed an increased proliferation percentage of Ki-67-positive tumor cells compared with the control group (group 1 versus group 3; Figures 3C and 3D). Taken together, these results demonstrated the reversion of cisplatin resistance by ectopic UCA1 expression *in vivo*.

UCA1 Targets miR-143 to Negatively Interact with miR-143

Up to now, accumulating evidence indicated that lncRNAs exerted their functions by interacting with miRNAs. Therefore, to investigate the effect of UCA1 on the expression of miRNAs, the bioinformatics prediction analysis was performed using the miRcode online website. As shown in Figure 4A, miR-143 harbors a complementary binding sequence to UCA1.

$p < 0.01$), suggesting that miR-143 is a UCA1-targeting miRNA. These outcomes indicated that the interaction of UCA1 and miR-143 was realized by the putative binding site.

Next, we measured the levels of miR-143 expression in ovarian cancer patient tissues and cell lines. As shown in Figure 4D, lower miR-143 expression was observed in cisplatin-resistant ovarian cancer tissues compared with that in cisplatin-sensitive ovarian cancer tissues. The expression of miR-143 was obviously decreased in cisplatin-resistant cells compared to that in cisplatin-sensitive cells, indicating the opposite result of UCA1 expression (Figure 4E; $p < 0.01$).

Subsequently, the effect of UCA1 on miR-143 expression was also observed in ovarian cancer cells. The results manifested that knock-down or overexpression of UCA1 significantly affected miR-143 expression (Figures 5A and 5B; $p < 0.01$). We further performed

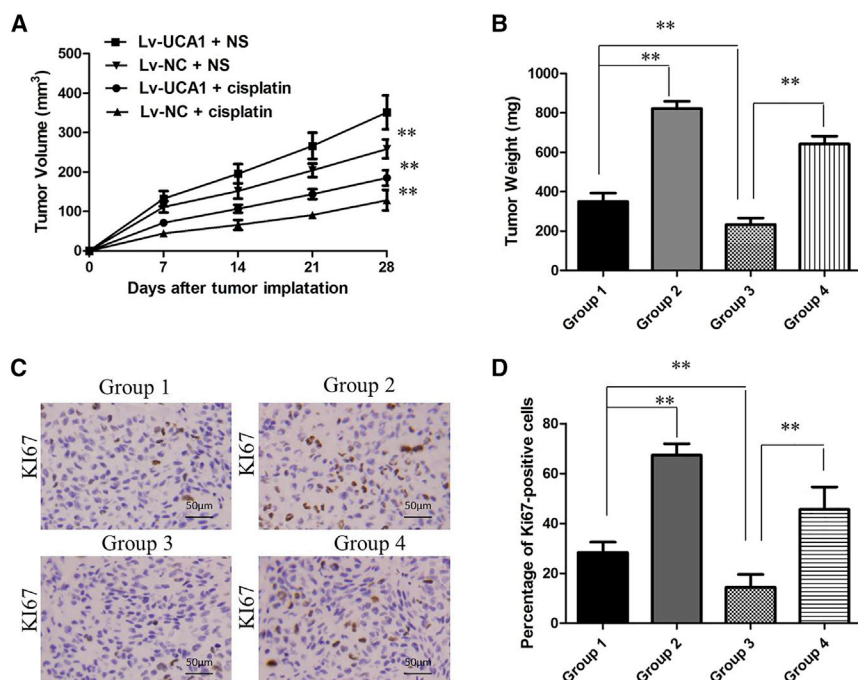


Figure 3. IncRNA UCA1 Promotes Cisplatin Resistance *In Vivo*

(A) Photographs of tumors that developed in xenograft transplanted nude mouse tumor models treated orally with once daily cisplatin or NS as control for 4 weeks in different groups. The group settings were as follows: group 1, Lv-UCA1-transfected cells + cisplatin; group 2, Lv-UCA1-transfected cells + NS; group 3, Lv-NC-transfected cells + cisplatin; and group 4, Lv-NC-transfected cells + NS. (B) Weights of tumors that developed in xenografts from different groups. ** $p < 0.01$ compared to respective groups. (C) IHC analysis of expression levels of Ki-67 in xenografts from different groups. (D) The percentage of Ki-67-positive cells in xenografts from different groups. All tests were performed at least three times. Data were expressed as mean \pm SD. ** $p < 0.01$.

rescue assays to confirm how the UCA1/miR-143 pathway modulated cisplatin resistance in ovarian cancer cells. We transfected miR-143 mimics and inhibitor into ovarian cancer cell lines, and the proliferation curves were determined. Our results showed that miR-143 overexpression markedly inhibits the cell growth in cisplatin-resistant cells when compared with cells transfected with miR-NC, whereas cisplatin-sensitive cells transfected with miR-143 inhibitor grew at a dramatically higher rate compared with controls (Figures 5C–5F; $p < 0.01$). Collectively, these data indicate that the UCA1/miR-143 pathway contributes to cisplatin resistance.

FOSL2 Is a Direct Target of miR-143

To investigate the molecular mechanism and genes targeted by miR-143, we used four target gene prediction websites (DIANA-microT, miRDB, TargetMiner, and miRanda) to predict potential target genes of miR-143. The results demonstrated that FOSL2 was a candidate target of miR-143 (Figure 6A). To further validate the inference, a WT or mutant FOSL2 3' UTR luciferase reporter vector was conducted. FOSL2-WT or FOSL2-MUT was co-transfected with miR-143 mimics or NC into cells. The relative luciferase activity was remarkably reduced in cells co-transfected with the FOSL2-WT luciferase reporter and miR-143 mimic than in the NC cells. However, inhibitory effects were abolished when 3' UTRs that contained both mutant-binding sites were co-transfected with miR-143, confirming that FOSL2 is a target of miR-143 (Figure 6B; $p < 0.01$).

We examined FOSL2 expression in ovarian cancer patient tissues and cell lines. The results of qRT-PCR demonstrated that the FOSL2 mRNA was higher in cisplatin-resistant ovarian cancer tissues

compared with that in cisplatin-sensitive ovarian cancer tissues (Figure 6C; $p < 0.01$). The expression of FOSL2 was obviously increased in cisplatin-resistant cells compared to that in cisplatin-sensitive cells (Figure 6D; $p < 0.01$). Subsequently, the actual impact of miR-143 on FOSL2 expression was detected by immunoblotting assays. Our results showed that enforced expression of miR-143 significantly diminished protein expression of FOSL2 *in vitro* (Figure 6E).

Serum Exosomal UCA1 Level Is Upregulated in Cisplatin-Resistant Ovarian Cancer Patients

Finally, in our current study, we extracted exosomes from 56 serum samples from ovarian cancer patients who received cisplatin treatment. First, we characterized these vesicles by several methods, such as electron microscopy (Figure 7A) and western blot (Figure 7B). The high presence of the exosomal markers TSG101 and HSP70 confirmed the purity of isolated laryngeal squamous cell carcinoma (LSCC)-secreted exosomes in the serum. Our results showed that UCA1 expression is detectable in extracted serum exosomes and is more highly expressed in the cisplatin-resistant group than in the cisplatin-sensitive group (Figure 7C; $p < 0.01$). Furthermore, there was a significant inverse correlation between the expression levels of UCA1 and miR-143 in serum exosomes derived from ovarian cancer patients (Figure 7D; $r = -0.523$, $p < 0.001$). Altogether, these results indicate that exosomal UCA1 in serum is stable and can serve as a promising biomarker for cisplatin-resistant ovarian cancer patients.

DISCUSSION

Noncoding RNAs, including miRNAs, lncRNAs, and circular RNAs (circRNAs), have important roles in the regulation of gene expression, and they are involved in the development of a variety of human diseases, including cancer.^{7,8} Therefore, targeting lncRNAs and elucidating the underlying mechanisms of lncRNAs may improve diagnostic and therapeutic strategies for ovarian cancer.

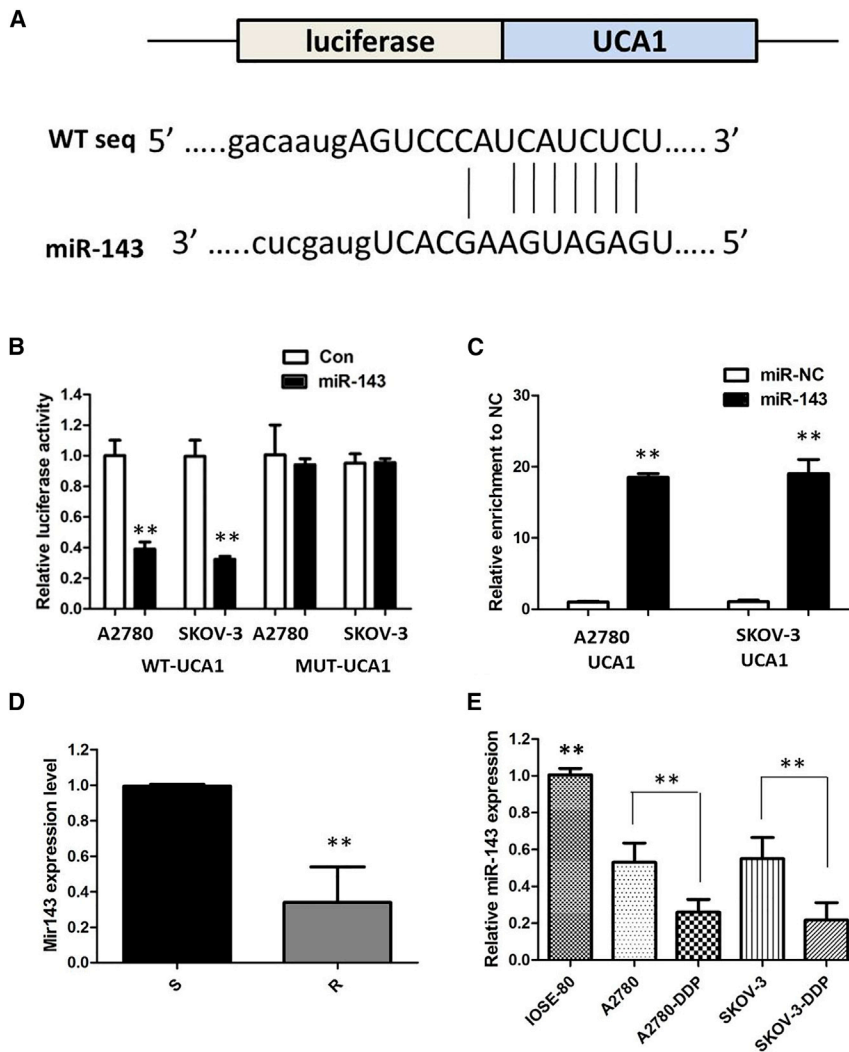


Figure 4. UCA1 Functions as a Molecular Sponge of miR-143 in Ovarian Cancer Cells

(A) StarBase v.2.0 results showing the sequence of UCA1 with highly conserved putative miR-143-binding sites. (B) miR-143 mimic considerably reduced the luciferase activity of the UCA1-WT luciferase reporter vector compared with NC, while miR-143 mimic did not have any impact on the luciferase activity of UCA1-MUT-transfected cells. (C) UCA1 and miR-143 simultaneously existed in the production precipitated by anti-AGO2. (D) Relative expression of miR-143 in the cisplatin-sensitive group and the cisplatin-resistant group in ovarian cancer patients. (E) Relative expression of miR-143 in a panel of ovarian cancer cell lines. All tests were performed at least three times. Data were expressed as mean \pm SD. ** $p < 0.01$.

cell carcinoma,¹⁰ melanoma,¹¹ gastric cancer,¹² and breast cancer.¹³ In agreement with these studies, we found that UCA1 overexpression contributed to ovarian cancer cells' cisplatin resistance. Upregulated UCA1 expression was observed in cisplatin-resistant ovarian cancer patients compared with that in cisplatin-sensitive ovarian cancer patients. To further validate the relationship between UCA1 expression level and cisplatin resistance, we performed loss-of-function studies by knocking down UCA1 in two cisplatin-resistant ovarian cancer cell lines, A2780-DDP and SKOV-3-DDP. Meanwhile, we upregulated the UCA1 expression in cisplatin-sensitive ovarian cancer cells by establishing UCA1-overexpressing cell lines. Suppression of UCA1 significantly reduced cell growth and promoted cell apoptosis of cisplatin-resistant cells in the presence of 4 μ g/mL cisplatin, compared with NC-transfected cells. However, UCA1 overexpression promoted the cisplatin-induced cell apoptosis and cell mobility of cisplatin-sensitive cells under cisplatin treatment.

Previously, it has been shown that UCA1 is overexpressed in various cancers and that UCA1 overexpression was significantly correlated with high-grade cancers, indicating that UCA1 may play an oncogenic role in cancers.⁹ Thus far, the role of UCA1 in the cisplatin resistance of ovarian cancer has not been elucidated. The present study showed that UCA1 is upregulated in cisplatin-resistant cells and patient tissues. Specifically, we also showed mechanistically that UCA1 provokes cisplatin resistance of ovarian cancer by sponging miR-143. Bioinformatics analysis predicted that there is a UCA1/miR-143/FOSL2 axis in the cisplatin resistance of ovarian cancer. Dual-luciferase reporter system and RIP assay validated the direct interaction of UCA1, miR-143, and FOSL2. Thus, our observations unravel a novel therapeutic strategy against cisplatin resistance by targeting the UCA1/miR-143 pathway.

The lncRNA UCA1 is generally regarded as an oncogene, and it is usually highly expressed in a variety of cancers, such as oral squamous

A growing volume of literature has proposed that lncRNAs mainly act as miRNA sponges to exert their post-transcriptional functions as competing endogenous RNAs (ceRNAs), which is more effective than the traditional anti-miRNA approach. Bioinformatics analysis (Starbase 2.0, RNA22) of miRNA recognition sequences on UCA1 revealed the presence of more than 30 miRNA-binding sites. Among them, miR-143 stood out through detailed survey. To further confirm the underlying molecular mechanisms involved, we performed the RIP and luciferase assays, and we found the direct binding ability of the miR-143 response elements on the full-length UCA1 transcript. Compared to lncRNAs, miRNAs have been well studied. Many studies have documented that dysregulation of miRNAs is closely associated with tumorigenesis. miRNAs inhibit target protein translation by interacting with the 3' UTRs of target

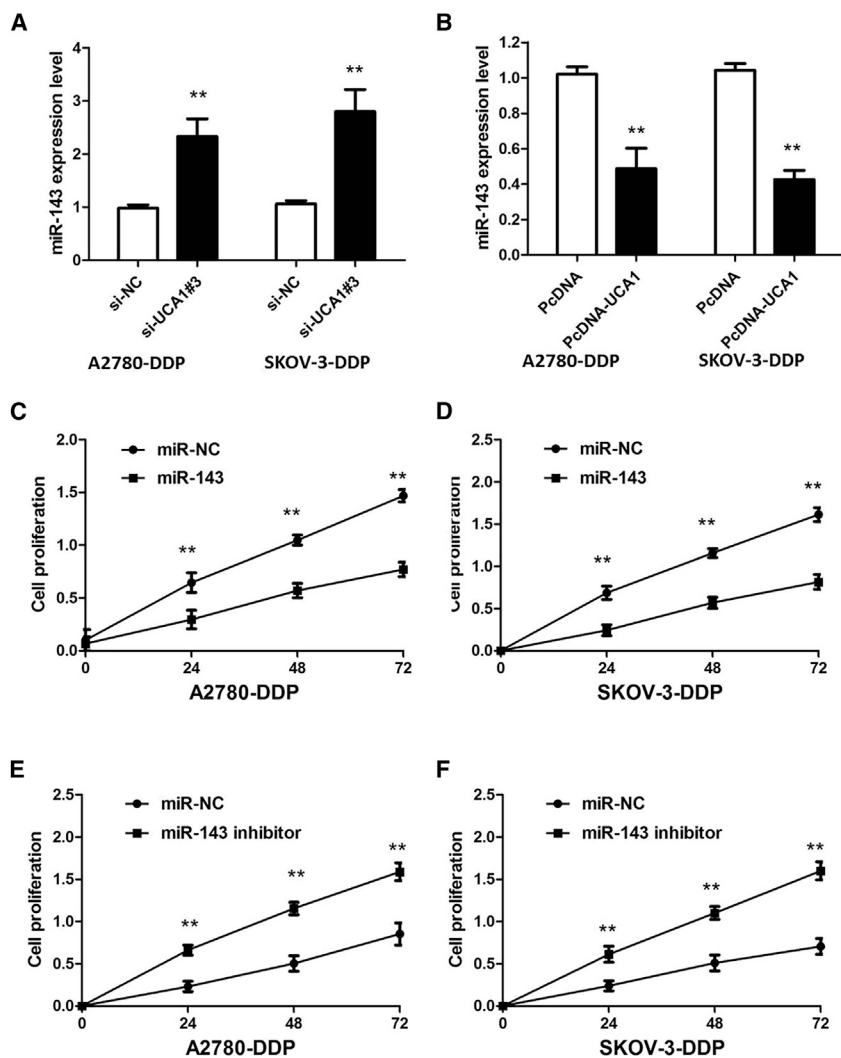


Figure 5. The effect of UCA1 on miR-143 Expression

(A) Silencing of UCA1 increased the expression level of miR-143 in A2780-DDP and SKOV-3-DDP cells. (B) Overexpression of UCA1 decreased the expression level of miR-143 in A2780 and SKOV-3 cells. (C) CCK-8 assay showing miR-143 overexpression markedly inhibits the cell proliferation of A2780-DDP cells in the presence of 4 $\mu\text{g}/\text{mL}$ cisplatin. (D) CCK-8 assay showing miR-143 overexpression markedly inhibits the cell proliferation of SKOV-3 cells in the presence of 4 $\mu\text{g}/\text{mL}$ cisplatin. (E) CCK-8 assay showing miR-143 inhibitor promoted the proliferation of A2780 cells in the presence of 4 $\mu\text{g}/\text{mL}$ cisplatin. (F) CCK-8 assay showing miR-143 inhibitor promoted the proliferation of SKOV-3 cells in the presence of 4 $\mu\text{g}/\text{mL}$ cisplatin. All tests were performed at least three times. Data were expressed as mean \pm SD. ** $p < 0.01$.

multiple types of cells and participate in intercellular communication by transmitting intracellular cargoes.^{16–19} lncRNAs could be protected from degradation in the circulation by exosomes and transferred between cancer cells, transmitting signals and phenotypes via exosomes.^{20–23} However, the functions of exosomal lncRNAs derived from ovarian cancer cells are still unknown. In this study, we found that UCA1 expression is detectable in the extracted serum exosomes of ovarian cancer patients and is more highly expressed in the cisplatin-resistant group than in the cisplatin-sensitive group.

Conclusions

In summary, our study reports that UCA1 contributes to the cisplatin resistance of ovarian cancer patients. Mechanistically, UCA1 functions as a molecular sponge to downregulate miR-143,

thereby resulting in partial abolition of the translational repression of its target gene FOSL2 in ovarian cancer cells. These findings illustrate a novel mechanism for understanding cisplatin resistance in ovarian cancer, and they suggest that UCA1/miR-143 has a potential therapeutic value for the treatment of cisplatin resistance in ovarian cancer patients.

MATERIALS AND METHODS

Clinical Specimens

The 56 paired ovarian cancer tissues and matched adjacent normal tissues were obtained from the Affiliated Hospital of Jining Medical University between 2010 and 2017. Tumor specimens and corresponding adjacent normal tissues were collected and stored in liquid nitrogen until use. For exosome purification, serum samples were collected from these 56 patients. Patients with progressive disease during primary chemotherapy or those who had recurrent disease within 6 months of completing primary chemotherapy were termed cisplatin resistant (R, $n = 32$). Patients with recurrence beyond

mRNAs.¹⁴ To date, miRNAs have been proven to act as either tumor suppressors or oncogenes in cancer initiation and the development of ovarian cancer.¹⁵

In this study, we found that miR-143 may play key roles in the regulation of ovarian cancer. We found that the miR-143 was significantly lower in cisplatin-resistant ovarian cancer tissue compared with cisplatin-sensitive ovarian cancer tissue. Further analysis showed that miR-143 can regulate FOSL2 protein expression by directly targeting the 3' UTR of FOSL2. The aberrantly downregulated miR-143 accompanied by the upregulated FOSL2 in cisplatin-resistant ovarian cancer may be potentially used for a novel therapeutic strategy against the cisplatin resistance of ovarian cancer patients.

In recent years, it has been accepted that lncRNAs could be protected from degradation in the circulation by exosomes and could be useful for monitoring cancer at the early stage. Exosomes are secreted from

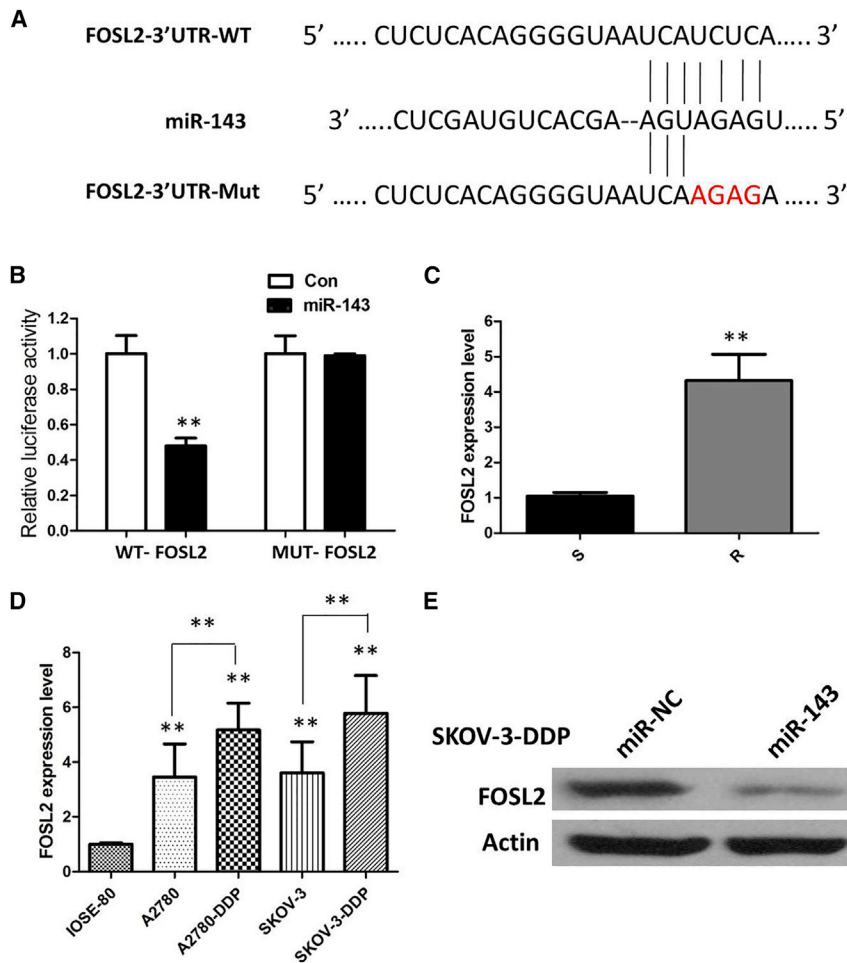


Figure 6. FOSL2 Is a Direct Target of miR-143

(A) Bioinformatics analysis revealed the predicted binding sites between FOSL2 and miR-143. (B) Luciferase reporter assay demonstrated miR-143 mimics significantly decreased the luciferase activity of FOSL2-WT in ovarian cancer cells. (C) The real-time PCR analysis was performed to determine the expression levels of FOSL2 in normal ovarian tissues and ovarian cancer tissues from cisplatin-resistant and cisplatin-sensitive patients. (D) Relative expression of FOSL2 in a panel of ovarian cancer cell lines. (E) Overexpression of miR-143 significantly decreased the protein expression of FOSL2 in SKOV-3-DDP cells. All tests were performed at least three times. Data were expressed as mean \pm SD. ** $p < 0.01$.

(HyClone, South Logan, UT, USA) with 10% fetal bovine serum (FBS; Invitrogen, Gaithersburg, MD, USA), while normal ovarian cells were maintained in 90% DMEM (Invitrogen) with high glucose and 10% FBS. All cell lines were cultured in 5% CO₂ at 37°C.

Expression Profile Analysis of lncRNAs

RNA expression profiling was performed using Agilent human lncRNA microarray version (v.)2.0 platform. Quantile normalization and subsequent data processing were performed using Agilent Gene Spring Software 11.5. Heatmaps representing differentially regulated genes were generated using Cluster 3.0 software. Exogenous RNAs developed by ERCC (External RNA Controls Consortium) were used as controls.

The exosomal lncRNA microarray process was performed by KangChen Bio (Shanghai, China).

RNA Extraction and Real-Time qPCR

Extraction of RNA from the exosome pellets was performed using the commercial miRNeasy Serum/Plasma kit (QIAGEN, Waltham, MA), according to the manufacturer's protocol. All RNA elution steps were carried out at 12,000 $\times g$ for 15 s, and the RNA was finally eluted in 15 μ L RNase-free ultra-pure water. Total RNA was extracted from tissues and cells by using Trizol reagent (Invitrogen, Carlsbad, CA, USA), according to the protocol of the manufacturer. RNA concentrations were detected by 260/280-nm absorbance using the Nanodrop spectrophotometer (ND-100; Thermo Scientific, Waltham, MA). SYBR Premix Ex Taq and TaqMan gene expression assays (Applied Biosystems, Foster City, CA, USA) were used to detect expression levels of lnc-UCA1, NR2C2, and GAPDH. TaqMan MicroRNA Reverse Transcription kit and Taqman Universal Master Mix II (Applied Biosystems) were used to detect miR-143 and U6 expressions. Relative expression values were normalized and calculated to represent fold change in gene expression using relative quantification as $2^{-\Delta\Delta CT}$.

6 months or without recurrence were termed cisplatin sensitive (S, $n = 24$). All of the cancer samples analyzed were serous ovarian cancer, which were obtained from the primary untreated tumors. In all of the cases, the diagnoses were confirmed by two experienced pathologists, which were done in accordance with the principles laid down in the latest World Health Organization Classification. Informed consent was also obtained from all of the patients, and the study was approved by the Medical Ethics Committee of the Affiliated Hospital of Jining Medical University. The research was carried out in accordance with the World Medical Association Declaration of Helsinki.

Cell Lines

Human ovarian cancer cell lines (A2780 and SKOV-3) and normal ovarian epithelial cell line (IOSE-80) were purchased from ATCC (Manassas, VA, USA) and BNCC (Beijing, China), respectively. Resistant ovarian cancer cell lines cisplatin-resistant A2780 (A2780-DDP; Yuci Biotech, Jiangsu, China) and cisplatin-resistant SKOV-3 (SKOV-3-DDP; Xinyu Biotech, Shanghai, China) were induced by cisplatin (Sigma, St. Louis, MO, USA). Ovarian cancer cells were maintained in RPMI 1640 medium

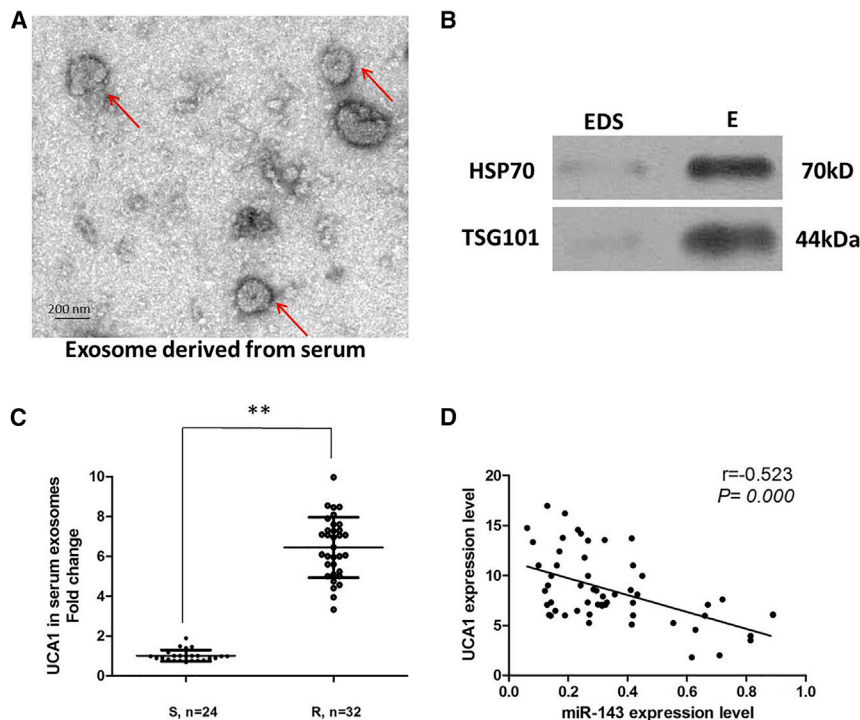


Figure 7. UCA1 Is Secreted into Exosomes Derived from the Sera of Ovarian Cancer Patients

(A) Representative image of exosome (indicated by red arrows), derived from the sera of ovarian cancer patients, detected from electron microscope. (B) The markers of exosome from purified serum exosome were analyzed by western blotting in exosomes (Es) and exosome-depleted supernatant (EDS). (C) qRT-PCR for the abundance of UCA1 in serum exosomes. The levels of UCA1 in serum exosomes from the cisplatin-resistant group were significantly higher than in the cisplatin-sensitive group. (D) In the exosomes extracted from the sera of ovarian cancer patients, the expression levels of UCA1 were negatively correlated with those of miR-143.

Cell Transfection

To construct the UCA1 overexpression plasmid, the full length of UCA1 cDNA sequence was amplified, cloned into pcDNA vector (Invitrogen), and sequenced, named as pcDNA-UCA1 (UCA1). Three specific siRNAs targeting UCA1 (si-UCA1#1, si-UCA1#2, and si-UCA1#3) and scrambled siRNA control (si-NC) were obtained from GenePharma (Shanghai, China). The lentivirus vectors containing UCA1 overexpression plasmid (Lv-UCA1) or NC vector (Lv-NC) were amplified and cloned by GeneChem (Shanghai, China). The miR-143 mimic (miR-143) and scrambled mimic control (miR-NC) were purchased from RiboBio (Guangzhou, China). All these plasmids and oligonucleotides were transfected into cells by Lipofectamine 2000 reagent (Invitrogen), following the manufacturer's instructions.

CCK-8 Assay

Cell proliferation was measured by the cell proliferation reagent Cell Counting Kit-8 (CCK-8; Roche, Basel, Switzerland). After cells were plated in the 96-well microtiter plates (Corning, Corning, NY, USA), 10 μ L CCK-8 reagent was added to each well at the time of harvest. Then, 2 h later, the absorbance was recorded at 450 nm to determine the cell viability.

Cell Apoptosis Analysis

For detecting apoptosis by flow cytometry, an annexin V-APC/DAPI double-staining kit (Thermo Fisher Scientific) was used to analyze cellular apoptosis. Cells were seeded in 6-well plates (5×10^5 cells/well) and then digested with trypsin (Gibco trypsin-EDTA, Thermo Fisher Scientific), washed with PBS three times, suspended in

500 μ L binding buffer, and then incubated with 5 μ L fluorescein isothiocyanate (FITC)-conjugated annexin V and 3 μ L propidium iodide (PI) for 15 min at room temperature in the dark. The stained cells were detected using the BD FACS Aria II flow cytometer (BD Biosciences, Hercules, CA, USA).

Tumor Xenograft Model

A total of 12 BALB/c female athymic mice at 4 weeks of age were housed and maintained in specific pathogen-free conditions. For injection, 1×10^7 SKOV-3 cells transfected with Lv-UCA1 or Lv-NC were suspended in 100 μ L PBS and injected subcutaneously into the flank. When tumors were palpable, the mice were randomized into treatment groups and control groups. Treatment lasted for 4 weeks until the xenograft tumor was stripped and the size was calculated. The experiments were performed in an observer-blinded and randomized manner.

Luciferase Reporter Assay

Sequences of potential binding sites of miR-143 in UCA1 full-length and FOSL2 3' UTR sequences and their mutant sequences were amplified by PCR and then cloned into a pmirGLO dual-luciferase Vector (Promega, Madison, WI, USA) to construct luciferase reporter vector (UCA1-WT and FOSL2-WT; GenePharma). Cells were seeded into 24-well plates in triplicate. After 24 h, the cells were transfected with UCA1-WT (or UCA1-MUT) or FOSL2-WT (or FOSL2-MUT) and miR-143 mimic or miR-NC using Lipofectamine 3000 (Invitrogen). Luciferase activity was measured in cell lysates 24 h after transfection using a Dual Luciferase Reporter System (Promega, Madison, WI, USA).

RIP Assay

RIP assay was performed using an EZ-Magna RiP Kit (Millipore, Billerica, MA, USA), in accordance with the manufacturer's instructions. Cells were lysed at 70%–80% confluence in RIP lysis buffer, and then they were incubated with magnetic beads conjugated with human anti-Ago2 antibody (Millipore) and normal mouse immunoglobulin G (IgG) control (Millipore) in RIP buffer. The RNAs in

the immunoprecipitates were isolated with Trizol reagent and analyzed by qRT-PCR.

Western Blotting Assay

Total proteins from cells, tissues, and exosome samples were extracted using a RIPA kit (Beyotime Biotechnology, Jiangsu, China). They were separated on polyacrylamide gels and transferred to polyvinylidene difluoride (PVDF) membranes. The membranes were incubated with anti-actin (Santa Cruz Biotechnology, Santa Cruz, CA, USA) and anti-FOSL2 (ab124830; Abcam, Cambridge, UK) antibodies at 4°C overnight, and they were then incubated with horseradish peroxidase-conjugated goat anti-rabbit or anti-mouse immunoglobulin G at room temperature for 1 h. To identify exosome markers, primary antibodies against TSG101 were purchased from Abcam (Cambridge, UK), and primary antibodies against Hsp 70 were obtained from Cell Signaling Technology (CST, Beverly, MA, USA). The secondary antibodies were F(ab)₂ fragments of donkey anti-mouse immunoglobulin or donkey anti-rabbit immunoglobulin linked to horseradish peroxidase (Jackson ImmunoResearch Laboratories, USA). Proteins were visualized using Pierce ECL Western Blotting substrate and autoradiography. Blots were analyzed using Quantity One 4.6.

Immunohistochemistry (IHC)

IHC analysis was performed using the manufacturer's instructions. Briefly, the slides were incubated with primary antibodies overnight at 4°C and then incubated with secondary antibodies at room temperature for 2 h. The expression was evaluated using a composite score obtained by multiplying the values of staining intensities (0, no staining; 1, weak staining; 2, moderate staining; and 3, strong staining) and the percentage of positive cells (0, 0%; 1, <10%; 2, 10%–50%; and 3, >50%).

Exosome Purification

Exosomes were extracted from serum samples using an ExoQuick precipitation kit (SBI, System Biosciences, Mountain View, CA), according to the manufacturer's instructions. Briefly, serum was thawed on ice and centrifuged at 3,000 × g for 15 min to remove cells and cell debris. Next, 250 μL supernatant was mixed with 63 μL ExoQuick precipitation kit and incubated at 4°C for 30 min, followed by centrifugation at 1,500 × g for 30 min. Then, the supernatant was removed by careful aspiration, followed by another 5 min of centrifugation to remove the residual liquid. The exosome-containing pellet was subsequently re-suspended in 250 μL PBS. Exosomes were measured for their protein content using a BCA protein assay kit (Pierce, Rockford, IL, USA). Electron microscopy was applied to characterize the vesicles floated in PBS.

Statistical Analysis

All the data were expressed as mean ± SD, and the statistical analyses were performed using GraphPad Prism (version 7.0, La Jolla, CA, USA). Two-sided Student's t test, χ^2 test, or Wilcoxon test was conducted to measure the differences between groups. $p < 0.05$ was considered to have statistical significance. The datasets supporting

the conclusions of this article are included within the article and its additional files.

SUPPLEMENTAL INFORMATION

Supplemental Information can be found online at <https://doi.org/10.1016/j.omtn.2019.05.007>.

AUTHOR CONTRIBUTIONS

X.C. performed primer design and experiments. Z.L. and H.N. contributed flow cytometry assay and animal experiments. Q.Q. and S.Y. collected and classified the human tissue samples. Q.W., C.Y., and Z.W. contributed to RT-PCR and qRT-PCR. Z.J. and X.W. analyzed the data. A.Y. and X.C. wrote the paper. All authors read and approved the final manuscript.

CONFLICTS OF INTEREST

The authors declare no competing interests.

ACKNOWLEDGMENTS

The present study was approved by the Institutional Review Board of the Affiliated Hospital of Jining Medical University. We received consent forms from individual patients who participated in this study. The consent forms will be provided upon request.

REFERENCES

- Vaughan, S., Coward, J.L., Bast, R.C., Jr., Berchuck, A., Berek, J.S., Brenton, J.D., Coukos, G., Crum, C.C., Drapkin, R., Etemadmoghadam, D., et al. (2011). Rethinking ovarian cancer: recommendations for improving outcomes. *Nat. Rev. Cancer* 11, 719–725.
- Vargas-Hernández, V.M., Moreno-Eutimio, M.A., Acosta-Altamirano, G., and Vargas-Aguilar, V.M. (2014). Management of recurrent epithelial ovarian cancer. *Gland Surg.* 3, 198–202.
- Gutschner, T., and Diederichs, S. (2012). The hallmarks of cancer: a long non-coding RNA point of view. *RNA Biol.* 9, 703–719.
- Xue, M., Chen, W., and Li, X. (2016). Urothelial cancer associated 1: a long noncoding RNA with a crucial role in cancer. *J. Cancer Res. Clin. Oncol.* 142, 1407–1419.
- Yang, Y.T., Wang, Y.F., Lai, J.Y., Shen, S.Y., Wang, F., Kong, J., Zhang, W., and Yang, H.Y. (2016). Long non-coding RNA UCA1 contributes to the progression of oral squamous cell carcinoma by regulating the WNT/ β -catenin signaling pathway. *Cancer Sci.* 107, 1581–1589.
- Nie, W., Ge, H.J., Yang, X.Q., Sun, X., Huang, H., Tao, X., Chen, W.S., and Li, B. (2016). LncRNA-UCA1 exerts oncogenic functions in non-small cell lung cancer by targeting miR-193a-3p. *Cancer Lett.* 371, 99–106.
- Lee, B., Mazar, J., Aftab, M.N., Qi, F., Shelley, J., Li, J.L., Govindarajan, S., Valerio, F., Rivera, I., Thurn, T., et al. (2014). Long noncoding RNAs as putative biomarkers for prostate cancer detection. *J. Mol. Diagn.* 16, 615–626.
- Cesana, M., Cacchiarelli, D., Legnini, I., Santini, T., Sthandier, O., Chinappi, M., Tramontano, A., and Bozzoni, I. (2011). A long noncoding RNA controls muscle differentiation by functioning as a competing endogenous RNA. *Cell* 147, 358–369.
- Yang, Y.N., Zhang, R., Du, J.W., Yuan, H.H., Li, Y.J., Wei, X.L., Du, X.X., Jiang, S.L., and Han, Y. (2018). Predictive role of UCA1-containing exosomes in cetuximab-resistant colorectal cancer. *Cancer Cell Int.* 18, 164.
- Fang, Z., Zhao, J., Xie, W., Sun, Q., Wang, H., and Qiao, B. (2017). LncRNA UCA1 promotes proliferation and cisplatin resistance of oral squamous cell carcinoma by suppressing miR-184 expression. *Cancer Med.* 6, 2897–2908.
- Wei, Y., Sun, Q., Zhao, L., Wu, J., Chen, X., Wang, Y., Zang, W., and Zhao, G. (2016). LncRNA UCA1-miR-507-FOXM1 axis is involved in cell proliferation, invasion and G0/G1 cell cycle arrest in melanoma. *Med. Oncol.* 33, 88.

12. Wang, Z.Q., He, C.Y., Hu, L., Shi, H.P., Li, J.F., Gu, Q.L., Su, L.P., Liu, B.Y., Li, C., and Zhu, Z. (2017). Long noncoding RNA UCA1 promotes tumour metastasis by inducing GRK2 degradation in gastric cancer. *Cancer Lett.* 408, 10–21.
13. Tuo, Y.L., Li, X.M., and Luo, J. (2015). Long noncoding RNA UCA1 modulates breast cancer cell growth and apoptosis through decreasing tumor suppressive miR-143. *Eur. Rev. Med. Pharmacol. Sci.* 19, 3403–3411.
14. Lin, P., Wen, D.Y., Li, Q., He, Y., Yang, H., and Chen, G. (2018). Genome-Wide Analysis of Prognostic lncRNAs, miRNAs, and mRNAs Forming a Competing Endogenous RNA Network in Hepatocellular Carcinoma. *Cell. Physiol. Biochem.* 48, 1953–1967.
15. Selbach, M., Schwanhäusser, B., Thierfelder, N., Fang, Z., Khanin, R., and Rajewsky, N. (2008). Widespread changes in protein synthesis induced by microRNAs. *Nature* 455, 58–63.
16. Tkach, M., and Théry, C. (2016). Communication by extracellular vesicles: where we are and where we need to go. *Cell* 164, 1226–1232.
17. Valenti, R., Huber, V., Iero, M., Filipazzi, P., Parmiani, G., and Rivoltini, L. (2007). Tumor-released microvesicles as vehicles of immunosuppression. *Cancer Res.* 67, 2912–2915.
18. Gezer, U., Özgür, E., Cetinkaya, M., Isin, M., and Dalay, N. (2014). Long non-coding RNAs with low expression levels in cells are enriched in secreted exosomes. *Cell Biol. Int.* 38, 1076–1079.
19. Sun, Z., Wang, L., Dong, L., and Wang, X. (2018). Emerging role of exosome signaling in maintaining cancer stem cell dynamic equilibrium. *J. Cell. Mol. Med.* 22, 3719–3728.
20. Cheng, L., Sharples, R.A., Scicluna, B.J., and Hill, A.F. (2014). Exosomes provide a protective and enriched source of miRNA for biomarker profiling compared to intracellular and cell-free blood. *J. Extracell. Vesicles* 3, 23743.
21. Shah, S., Wittmann, S., Kilchert, C., and Vasiljeva, L. (2014). lncRNA recruits RNAi and the exosome to dynamically regulate *pho1* expression in response to phosphate levels in fission yeast. *Genes Dev.* 28, 231–244.
22. Boukouris, S., and Mathivanan, S. (2015). Exosomes in bodily fluids are a highly stable resource of disease biomarkers. *Proteomics Clin. Appl.* 9, 358–367.
23. Denzer, K., Kleijmeer, M.J., Heijnen, H.F., Stoorvogel, W., and Geuze, H.J. (2000). Exosome: from internal vesicle of the multivesicular body to intercellular signaling device. *J. Cell Sci.* 113, 3365–3374.